



# Inhibition of thin polystyrene film dewetting via phase separation

Xue Li, Yanchun Han\*, Lijia An\*

*State Key Laboratory of Polymer Physics and Chemistry, Changchun Institute of Applied Chemistry, Chinese Academy of Sciences, No 5625 Renmin Street, Changchun 130022, People's Republic of China*

Received 19 March 2003; received in revised form 28 June 2003; accepted 30 June 2003

## Abstract

By addition of a small amount of poly(methyl methacrylate) (PMMA) into polystyrene (PS), we present a novel approach to inhibit the dewetting process of thin PS film through phase separation of the off-critical polymer mixture (PS/PMMA). Owing to the preferential segregation of PMMA to the solid  $\text{SiO}_x$  substrate, a nanometer thick layer, rich in PMMA phase, is formed. It is this diffusive PMMA-rich phase layer near the substrate that alters the dewetting behavior of the PS film. The degree of inhibition of dewetting depends on the concentration and molecular weight of PMMA component. PMMA with low (15.9k) and intermediate (102.7k) molecular weight stabilizes the films more effectively than that with a higher molecular weight (387k).

© 2003 Elsevier Ltd. All rights reserved.

**Keywords:** Polystyrene; Poly(methyl methacrylate); Dewetting

## 1. Introduction

The stability and the wetting behavior of thin ( $< 100$  nm) liquid (e.g. polymer) films on a solid substrate are of technological and scientific importance in applications ranging from coatings, paints, dielectric layers, thin film lubrication, and microelectronic and optoelectronic devices to fundamental studies of multilayer adsorption and polymer diffusion [1–3]. However, synthetic polymer films often dewet from inorganic substrates. To avoid spontaneous pattern formation and the break-up of such films, an understanding of the wetting is required. The factors determining film stability, i.e. ensuring that the polymer wets the surface, require that the opposite phenomenon (dewetting) be also well understood [4]. Therefore, understanding and controlling the factors leading to thin film dewetting is of critical importance in obtaining uniform, continuous, defect-free, and stable coatings. However, in many applications, the films are composed of multicomponent polymer systems, such as paints, adhesives, and lubricants. Hence, it is also important to

investigate the stability and structure of a thin polymer film containing other component or additive [5].

For thin polymer blend films, many studies have been made in recent years [6–8]. It has been demonstrated that the behavior of polymer blend films is qualitatively different from that of polymer blends in the bulk. Because the blend is confined between two different interfaces (one toward the substrate and one toward the air) and generally a preferential segregation of one component or phase of the blend to the interfaces, the resulting segregation will break the compositional symmetry and a phenomenon called surface-directed spinodal decomposition can be induced. When the thickness of the polymer blend films is thinner than the characteristic spinodal wavelength, which is on the order of  $\sim 100$  nm, surface-directed spinodal decomposition is suppressed [9–17]. Because air surface prefers the lower surface energy phase, the substrate interfacial preference can change from one blend component to another when the nature of the substrate surface is changed [10–13,18]. Therefore, it has been concluded that the phase morphology and its time evolution in thin, phase-separated polymer films are governed by the complex interplay between phase-separation processes and the interactions of the polymer phases with the air and substrate. In immiscible polystyrene (PS)/PMMA system [19], the author had noted that during solvent casting it was also possible that a dewetting

\* Corresponding author. Tel.: +86-431-526-2175x2206; fax: 86-431-526-2126..

E-mail addresses: [yhan@ns.ciac.jl.cn](mailto:yhan@ns.ciac.jl.cn) (Y. Han), [ljan@ns.ciac.jl.cn](mailto:ljan@ns.ciac.jl.cn) (L. An).

mechanism existed when phase separation took place. In weakly incompatible deuterated PS/poly(*p*-methylstyrene) (dPS/PpMS) films [20], the surface morphology is controlled by interplay between phase separation and dewetting. Generally, a bicontinuous spinodal decomposition pattern in critical binary blend films and a droplet- or holelike surface morphology in off-critical blends were observed [15]. However, for a binary mixture of polymer A and polymer B, which B component has an affinity for the substrate interface and A for the air interface, only few papers reported the effects of phase separation on the dewetting properties of the binary mixture when the concentration of polymer B is very low.

It has been reported that the addition of small amount of diblock copolymer (0.05 volume fraction) to the PS can increase the polymer film stability [21]. Nanofillers, such as fullerene nanoparticles (buckyballs, C<sub>60</sub>) [22], carbon black and colloidal Si nanoparticle fillers [23] were introduced into the polymer films to inhibit the dewetting of thin polymer films. Recently, Mackay et al. [24] reported that a small mass concentration of poly(benzyl ether) dendrimer added to low molecular weight PS was found to inhibit the dewetting of a thin (~50 nm) PS film. Although the exact mechanism of dewetting retardation of dendrimer is unknown, the preferential segregation of dendrimers to the substrate surface by phase separation seems to be an important factor in film stabilization effect. Joshua et al. [25] also observed that the stability (wettability) of low molecular weight PS thin films on a silicon substrate was improved by the addition of high surface energy polyetherimide hyperbranched polymers (PEI HBPs).

In this paper, we demonstrate that the dewetting of polymer films can be inhibited through phase separation of a off-critical polymer mixture. This may be a simple and low-cost method of dewetting inhibition of the polymer films. As a model system, (PS)/poly(methyl methacrylate) (PMMA) blends were selected because this system had been studied intensively before, both in its phase separation behavior in thin films [19,26,27] and dewetting properties of PS films on the SiO<sub>x</sub> substrates [28–32] and the upper PS films on the PMMA layers [33,34].

## 2. Experimental

### 2.1. Materials

The samples of PS (noted as PS and NPS) were purchased from Nanjing University, P. R. China. The PMMA samples were purchased from the Aldrich Chemical Company and used as received. Their characteristics are shown in Table 1. The radius of gyration of the unperturbed chain was calculated by means of the following equation

$$R_g = (Nb^2/6)^{1/2} \quad (1)$$

Table 1  
Characteristics of PS and PMMA

Polymer	$M_w$	$M_n$	$M_w/M_n$	$2R_g$ (nm)	$T_g$ (°C)
PS	2.9k	2.8k	1.05	2.9	62
NPS	20.9k	20.3k	1.03	3.9	93
PMMA1	15.9k	12.9k	1.23	7.1	90
PMMA10	102.6k	48.3k	2.12	18.0	109
PMMA38	387k	104k	3.72	35.0	122

where  $N$  is the degree of polymerization and  $b$  is the average statistical segment length. For PS and PMMA,  $b_{PS} = 0.68$  nm and  $b_{PMMA} = 0.69$  nm, respectively. The glass transition temperatures ( $T_g$ ) of PS and PMMA were determined by differential scanning calorimetry (Perkin–Elmer DSC-2C) with a heating rate of 20 °C/min by twice scanning. The solvent toluene for spin-coating was analytical grade.

### 2.2. Film preparation

The polymer solutions were prepared by dissolving a mixture of PS and PMMA (w/w) with specific composition in toluene (1.0 wt%). The silicon wafer was cleaned with a mixed solution of concentrated H<sub>2</sub>SO<sub>4</sub> and H<sub>2</sub>O<sub>2</sub> (30%) (70/30 v/v) at 110 °C for 1 h, then rinsed in deionized water for several times and dried. The polymer solutions were filtered with a 0.22 μm Millipore membrane before spin-coating.

The blend films were prepared with a KW-4A precision spin-coater (Chemat Technology, Inc.) in a glove box. The spin-coating was carried out at 2000 rpm for 30 s at room temperature. All the prepared films were dried at 50 °C in vacuo for two days to remove remaining solvent completely. The film thickness was measured by ellipsometer. The average film thickness of the blend films was ca. 50 nm.

### 2.3. Observation of film morphology

The films were annealed under vacuum at 150 °C (above the glass transitions of the PS and PMMA) for various times. The morphologies of the annealed samples were imaged by a Leica optical microscopy in reflection mode. To avoid undesired effects associated with heating and cooling of one sample, different samples were used for each annealing time [24].

Atomic force microscopy (AFM) measurements were performed on SPA300HV with an SPI3800 controller, Seiko Instruments Industry, Co. Ltd. The images were taken with the contact mode and friction force microscopy (FFM) images were performed simultaneously with topographical imaging. For NPS and NPS/PMMA10 blend films, the dewetting behavior was observed directly with AFM equipped with a hot stage in vacuum.

## 2.4. X-ray photoelectron spectroscopy

The XPS was measured with VG ESCALAB MK at room temperature by using an Mg K $\alpha$  X-ray source ( $h\nu = 125.36$  eV) at 14 kV and 20 mA. The sample analysis chamber of the XPS instrument was maintained at a pressure of  $1 \times 10^{-7}$  Pa. All the C $_{1s}$  peaks were calibrated to the standard binding energy of 284.6 eV for neutral carbon in order to correct the charging energy shifts. A linear-background method removed the XPS background and the peaks analysis carried out by using the curve-fitting software.

## 3. Results and discussion

### 3.1. Influence of PMMA concentration on the thin PS film dewetting

When a pure low molecular weight PS film on a SiO $_x$  substrate was annealed at 150 °C (above the  $T_g$  of PS) for 50 min, the dewetting of the PS film (50 nm thick) took place and a Vorronoi tessellation pattern formed (Fig. 1). In order to understand the effect of phase separation on the PS film stability, a low concentration PMMA was added to the PS. Fig. 2 shows the dewetting behavior of PS/PMMA10 blends with PMMA10 content of 1.0, 5.0 and 10.0 wt%, respectively. For the films with PMMA10 content of 1.0 and 5.0 wt%, the films were annealed at 150 °C for 20 min, 50 min, and 2 h, respectively. For the films with 10.0 wt% PMMA10, the films were annealed at 150 °C for 20 min, 48 and 72 h, respectively. Compared with a pure PS film, Fig. 2(a)–(c) indicated that the addition of only 1.0 wt% PMMA10 to the PS film had caused an appreciable slowing down of the film dewetting process. The dewetting

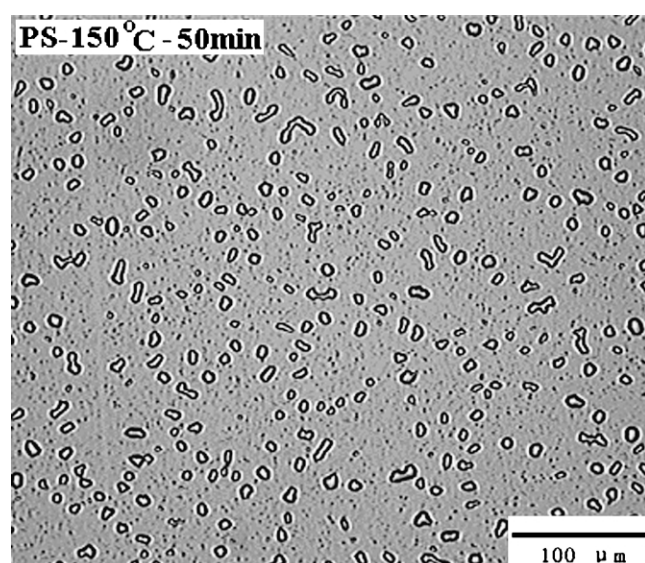


Fig. 1. Optical micrograph showing the dewetting pattern of a 50 nm low molecular weight PS film on SiO $_x$  substrate annealed at 150 °C for 50 min.

suppression was enhanced with the content of PMMA10 (Fig. 2(d)–(i)). By increasing the content of PMMA10 to 10.0 wt%, the PS/PMMA10 blend film did not dewet even annealing at 150 °C for 72 h (Fig. 2(g)–(i)). The AFM images insert in Fig. 2(i) indicated that the hole formation in the early stage of dewetting in the PS film with 10 wt% PMMA10 did not occur, i.e. the dewetting was completely inhibited when the content of PMMA10 was increased to 10.0 wt%. The phenomena are similar to the observations of Mackay et al. [24], who found that the addition of 10.0 wt% of the smallest generation dendrimer to a low molecular weight PS, dewetting could be retarded to a great extent though the origin of dewetting inhibition mechanism was not understood completely [24].

For a PS film with a low concentration of PMMA, it is expected that the dewetting inhibition of a PS/PMMA10 blend film is mainly caused by the preferential segregation of PMMA to the substrate. Since the PMMA component has a higher surface energy than that of PS, PMMA is expected to segregate to the SiO $_x$  substrate [19] and form a nanometer-thick diffusive layer, which changes the film structure and decreases the interfacial tension between the PS and the PMMA.

It has been shown that the surface structure of a spin-coated polymer blend thin film depends on the solubility of the two polymers in the common solvent and the surface energy of the substrate [19]. Toluene is a better solvent for PS than for PMMA. Hence, the PS-rich phase has a higher toluene content than the PMMA-rich phase [35]. PMMA is more quickly depleted from the solvent and solidifies first onto the substrate during spin-coating and leads to more PMMA-rich phases near the substrate [19]. The AFM height images of the spin-coated PS/PMMA10 films treated with cyclohexane [19,27] for 3 min (Fig. 3(a)–(c)) clearly show that the substrate were covered by PMMA-rich phase domains. The average domain sizes in Fig. 3(a)–(c) are about 70, 85 and 100 nm, respectively, and the domain distributions of the PMMA10 particles are relatively uniform. To further verify that the SiO $_x$  substrate surface was covered by PMMA-rich phase, XPS measurements of thin PS/PMMA (95/5, w/w) blend films before and after treatment with cyclohexane were performed (Fig. 4). The C $_{1s}$  peak at 288.4 eV, which is assigned to carbonyl carbon, was almost not observed (Fig. 4(a)). After the sample was treated with cyclohexane for 3 min, the XPS C $_{1s}$  spectrum shown in Fig. 4(b) is corresponding to the C $_{1s}$  of pure PMMA. This indicates that the substrate is covered by PMMA-rich phase. Compared to the structure of a pure PS film (air/PS/SiO $_x$ /Si), the structure of the film containing small amount PMMA has changed into air/PS-rich phase/PMMA-rich phase/SiO $_x$ /Si. To examine whether the substrate was covered or screened completely by PMMA10-rich phase or not, the friction images were also taken with AFM (Fig. 3(a'), (b') and (c')). When PMMA10 content was 1.0 wt%, the contrast in the friction image (Fig. 3(a')) indicated that the substrate was not covered by



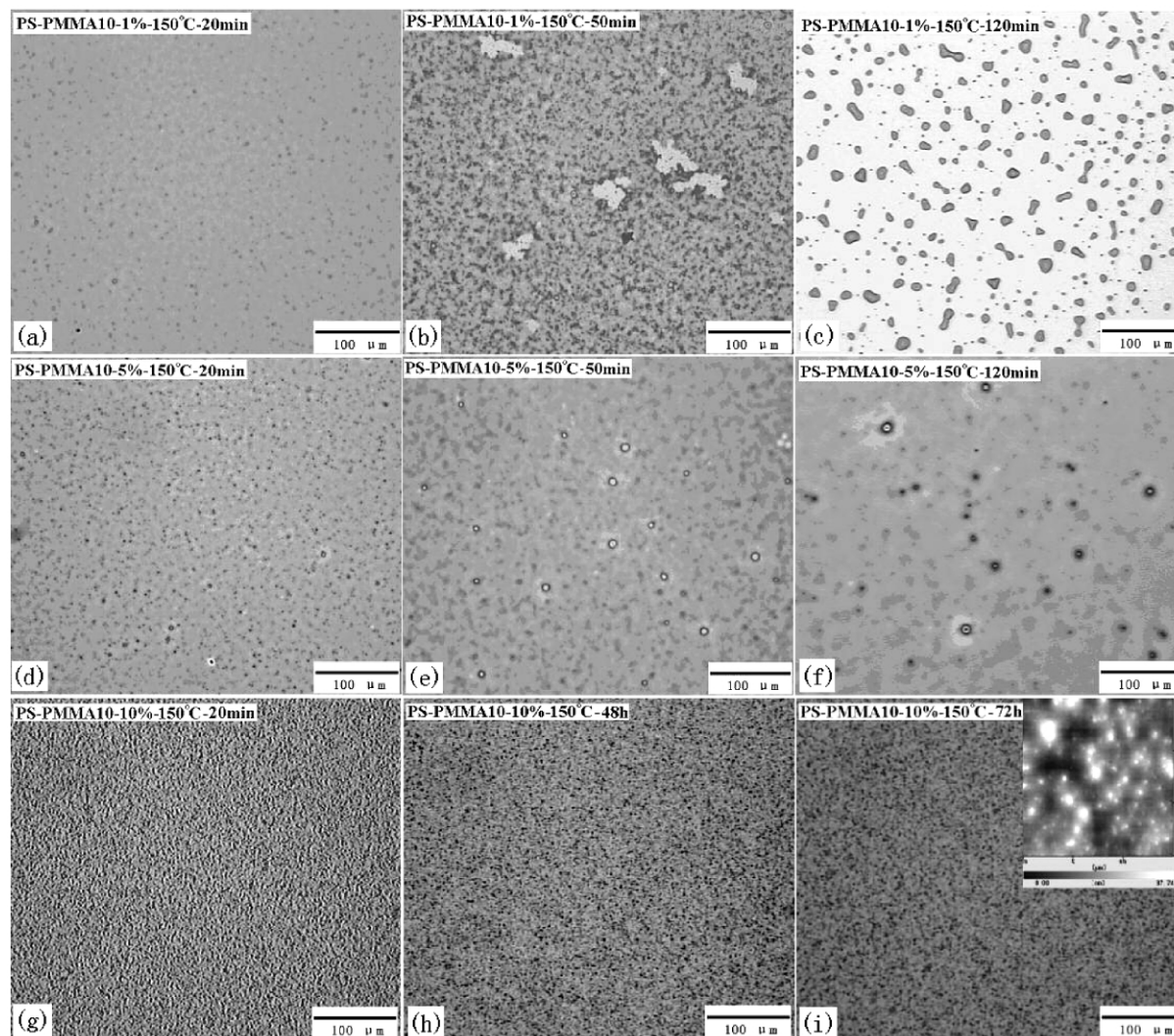


Fig. 2. The dewetting patterns of PS/PMMA10 blend films with different PMMA10 content. 1.0 wt% for (a)–(c) and the corresponding annealing time are 20, 50 min and 2 h, respectively. 5.0 wt% for (d)–(f) and the corresponding annealing time are 20, 50 min and 2 h, respectively. 10.0 wt% for (g)–(i) and the corresponding annealing time are 20 min, 48 and 72 h, respectively. All pictures were taken by reflection OM. Insert in (i) is the AFM image ( $15\ \mu\text{m} \times 15\ \mu\text{m}$ ,  $z\text{-range} = 37\ \text{nm}$ ) of the same film at a much higher magnification.

PMMA10-rich phase completely. When PMMA10 content increased to 5.0 or 10.0 wt%, the  $\text{SiO}_x$  substrate was covered or screened completely by small PMMA10-rich phase domains, i.e. the polymer–substrate interaction was changed from PS–substrate interaction for pure PS films into PMMA–substrate interaction for PS/PMMA10 blend film. Therefore, the dewetting of a blend film was inhibited. The inhibition extent is enhanced with the increase of PMMA10 content from 1.0 to 10.0 wt%.

In addition, the change of the film structure alters the surface roughness. It has been reported that surface roughness has the effect of enhancing polymer–substrate interaction [36]. The roughness of the PMMA10-rich phase layers in Fig. 3(a)–(c) are about 1.2, 2.7 and 5.0 nm, respectively. These values are larger than that of silicon substrate (ca. 0.2 nm) and may have attribution to the film stabilization [37].

The presence of a nanometer-thick PMMA-rich phase layer on the substrate can decrease the interfacial tension between PS and PMMA, which may change the stability of a thin liquid film. Provided that all PMMA10 is segregated to the  $\text{SiO}_x$  surface by phase separation, the thickness of the underlying PMMA10-rich phase layer is less than 5.0 nm if estimated from the PMMA10 content of the PS/PMMA10 blend film (from 1.0 to 10.0 wt%) due to the volume conservation. The thickness of the PMMA-rich phase layer measured by ellipsometer was about 8 nm after the PS/PMMA10 film with 10.0 wt% PMMA was etched with cyclohexane for 3 min. The thickness is less than  $2R_g$  (18.0 nm) of PMMA10. The PMMA10-rich phase layer is so thin that the PMMA10 chains at the  $\text{SiO}_x$  interface are not coils and may be stretched out straightly like reeds on the pond bed [38]. Hence, there will be more PMMA10 chains stretching into the PS-rich phase and make the interfacial

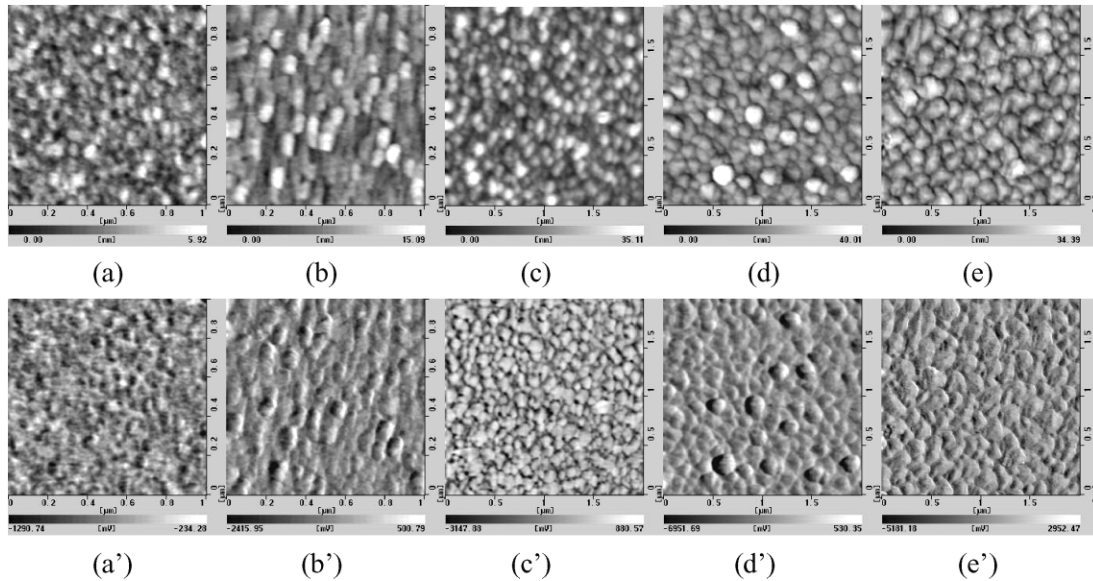


Fig. 3. AFM and FFM images showing the surface structures of PMMA-rich phase layer of PS/PMMA10 films after treatment with cyclohexane for 3 min. PMMA10 content: (a), (a') 1.0 wt%; (b), (b') 5.0 wt%; (c), (c'), (d), (d') (e), (e') 10.0 wt%. Annealing time: (a), (a'), (b), (b'), (c), (c') 0 h; (d), (d') 48 h; (e), (e') 72 h.

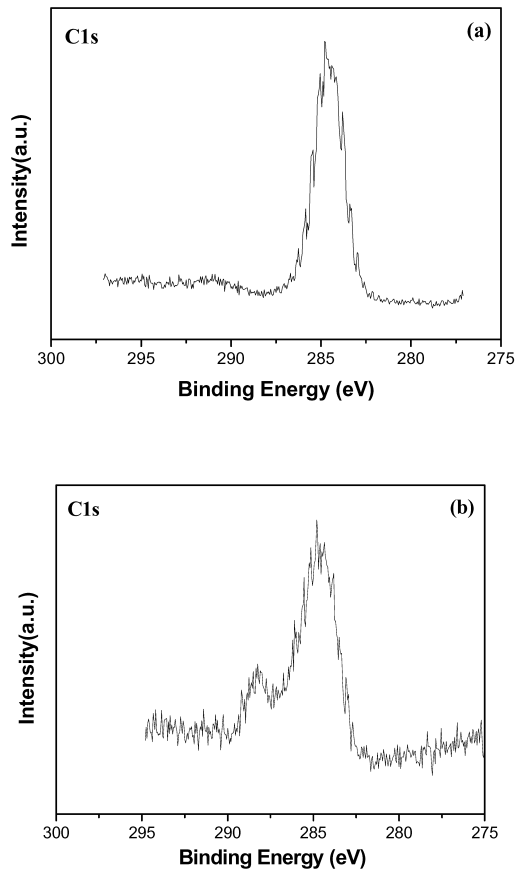


Fig. 4. XPS C1 s spectra of the PS/PMMA10 (95/5, w/w) thin films before (a) and after (b) treatment with cyclohexane for 3 min. The sample had been annealed at 150 °C for 50 min.

tension,  $\gamma_{\text{PS/PMMA}}$ , decrease. Thus, the driving force for dewetting will be lower [21]. The result of Sferazza et al. [39] also indicated that the effects of  $\text{SiO}_x$  substrate on the dewetting behavior of a PS film and a PS blend film are different. The attractive dispersion force of the  $\text{SiO}_x$  substrate, which can cause a pure PS film dewet, could stabilize the interface between a thin film of PS and a PMMA layer [39]. Therefore, the formation of a nanometer-thick diffusive layer, rich in PMMA, near the substrate surface was also postulated to be the main mechanism for dewetting inhibition.

To examine the effect of the molecular weight of PS on the dewetting inhibition of the PS films by phase separation, another high molecular weight PS (noted as NPS,  $M_w = 20.9\text{k}$ ) was used to prepare pure and blend films. The samples were observed directly by AFM equipped with

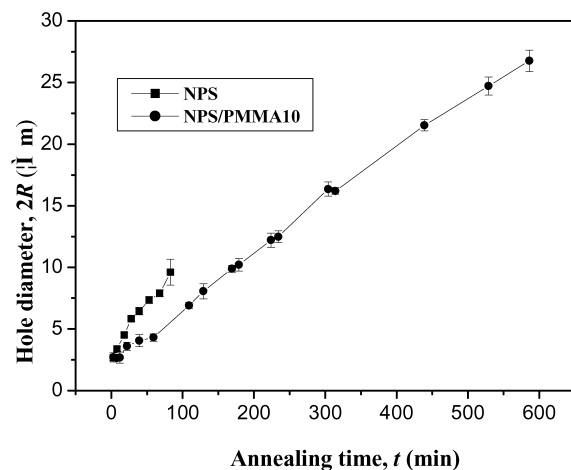


Fig. 5. Hole growth as a function of time at 150 °C for NPS and NPS/PMMA10 (4 wt%) films.



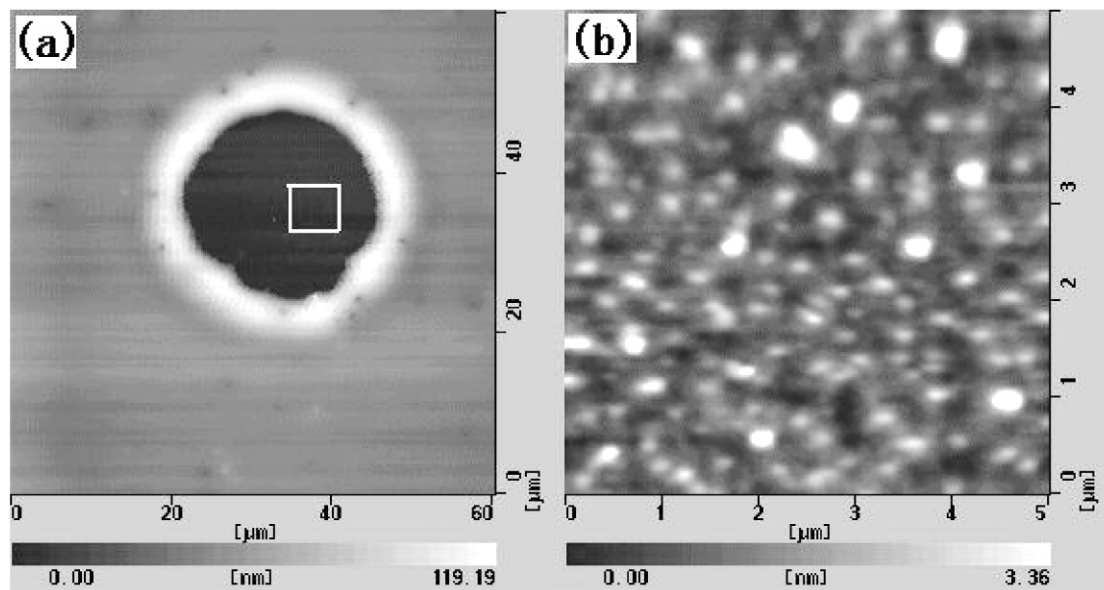


Fig. 6. AFM images of the topology of an isolated hole (a) and the hole floor (b) for the NPS/PMMA10 (4 wt%) film after 530 min at 150 °C in vacuum.

a hot stage. The growth of diameter of holes in the NPS film and NPS/PMMA10 (4 wt%) film are displayed in Fig. 5. Upon adding 4.0 wt% PMMA, the rate of hole growth was reduced greatly. A hole and the hole floor morphology for the blend sample (Fig. 6) indicated that the substrate was covered uniformly with PMMA-rich phase domains even annealed at 150 °C for 530 min. This rough PMMA-rich phase layer increases the viscous frictional force between PS and PMMA and decreases the rate of hole growth. Hence, the dewetting of the PS films can be inhibited by phase separation.

Dynamically, in terms of the collective modes of liquid/liquid dewetting [40], the decrease of the dewetting rate of the blend film can be attributed to the large viscosity of the PMMA-rich phase layer pinned onto the substrate [41]. As shown in Fig. 3(c)–(e), the AFM images of the etched PS/PMMA10 films having been annealed for 0, 48

and 72 h clearly illustrate that the nanometer thick PMMA-rich phase layer formed by PMMA segregating to the  $\text{SiO}_x$  substrate was still remained, the structure changes of PMMA-rich phase layer was slow during annealing.

### 3.2. Influence of molecular weight of PMMA on the thin PS film dewetting

In order to investigate the effect of the PMMA molecular weight on the PS dewetting behavior, PS blended with 10.0 wt% PMMA with  $M_{w, \text{PMMA}}$ , 15.9k, 102.6k and 387k, respectively, were chosen as three different model systems. Upon annealing at 150 °C for 2 h, PS/PMMA1 and PS/PMMA38 films were nearly smooth on a large scale and did not exhibit any dewetting. After annealing for 48 h, the PS/PMMA1 film did not dewet the substrate (Fig. 7(a)) as that of PS/PMMA10 film. However, white areas on the

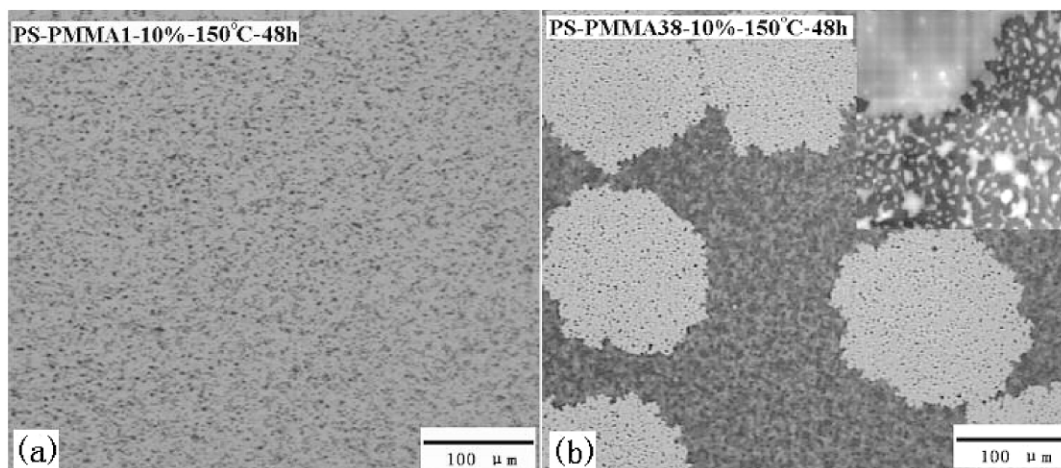


Fig. 7. The OM pictures of PS/PMMA films with 10.0 wt% PMMA annealed at 150 °C for 48 h. (a) PS/PMMA1; (b) PS/PMMA38. Insert in (b) is the AFM image (15 μm × 15 μm, z-range = 108 nm) taken from crossover area from non-dewetted to dewetted areas in OM micrograph.

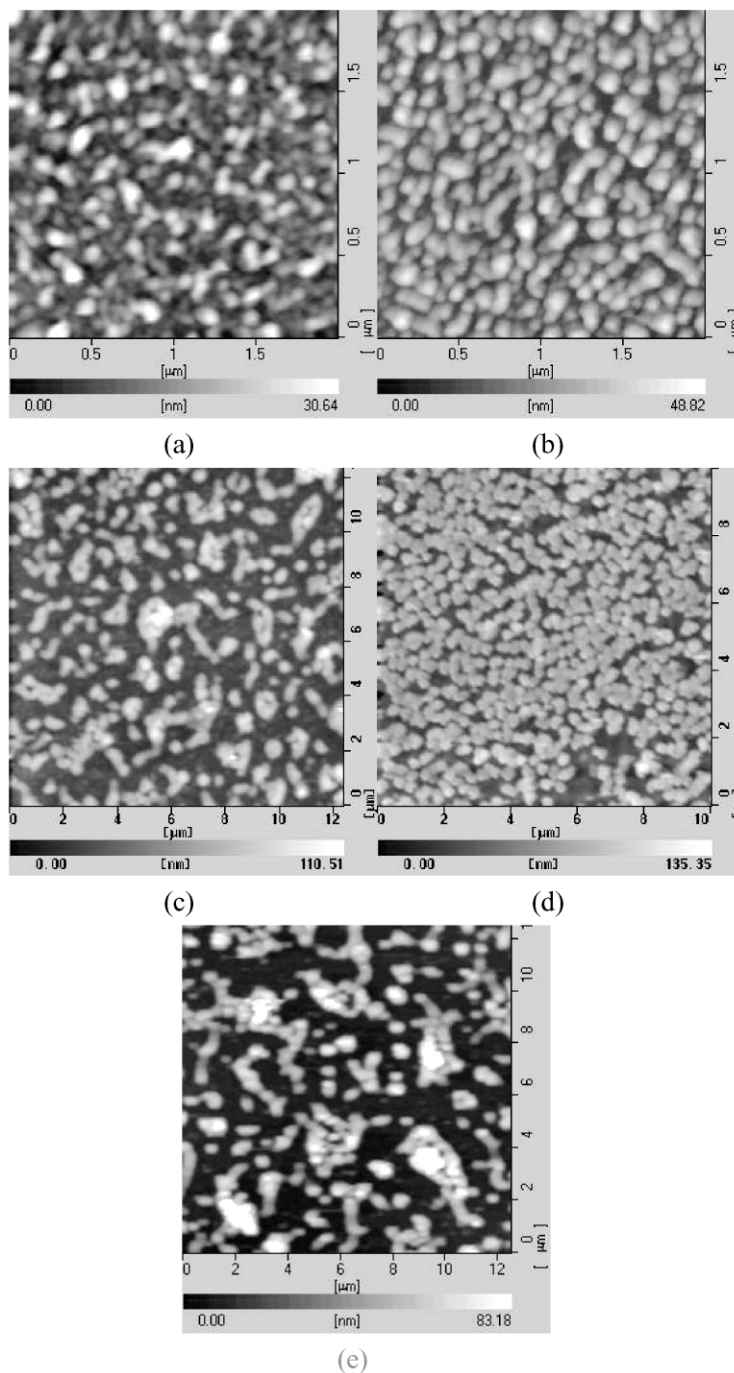


Fig. 8. AFM images showing the structures of PMMA-rich phase layer of PS/PMMA38 with 10.0 wt% films after annealing for (a) 0 h; (b) 12 h; (c) and (d) 48 h; (e) 72 h. The samples were etched with cyclohexane for 3 min. The images of (c) and (d) were taken from the areas corresponding to dewetted and non-dewetted areas in OM pictures in Fig. 7(b).

surface of PS/PMMA38 film were observed (Fig. 7(b)). Insert in Fig. 7(b) shows the AFM height image scanned at the crossover region from white to dark areas in OM micrograph. It can be seen clearly that the film in white areas had dewetted and formed discrete domains. When annealing further, the white areas grew up to sufficient size and impinged on adjacent white areas, and finally the whole film dewetted. These results reveal that the stabilization of PS/PMMA films decrease with increase PMMA molecular weight.

To investigate the dewetting mechanisms of the PS/PMMA38 films, Fig. 8 shows the AFM images of the films which were annealed for 0, 12, 48 and 72 h and then treated with cyclohexane. Similar to the result of a spin-coated PS/PMMA10 film, the  $\text{SiO}_x$  substrate was completely covered by small PMMA38-rich phase particles before annealing (Fig. 8(a)). Upon annealing for 12 h, the PMMA-rich phases began to coalesce (Fig. 8(b)). After annealing for 48 h, the structure change of the PMMA38-rich phase

layer next to the substrate was evident. In the dewetted or white areas in Fig. 7(b), the PMMA38-rich phase layer had become into large aggregates (Fig. 8(c)) and the SiO<sub>x</sub> substrate was mostly exposed out (about 62%). The PS chains may connect with exposed SiO<sub>x</sub> substrate and the large PMMA38 aggregates may become into nucleation sites, hence dewetting occurred within surface regions free of PMMA38-rich phase. In the non-dewetted or dark areas in Fig. 7(b), the PMMA38-rich phase layer had become bicontinuous-like structures (Fig. 8(d)). However, the area fraction of the exposed SiO<sub>x</sub> substrate was about 36% and may not be large enough to induce film dewetting. Therefore, the film in this region did not dewet. With the increase of the annealing time, the bicontinuous-like PMMA38-rich phase would coarsen and become into the large aggregates (Fig. 8(e)) and cause the whole film dewet. Therefore, the structure change of the PMMA38-rich phase layer next to the substrate resulted in the difference in inhibition of dewetting between PMMA38 and PMMA10.

The difference of the structure change of the PMMA-rich phase layer between the two kinds of films with different PMMA molecular weight (PMMA10 and PMMA38) may be mainly induced by entropic effect. The results of Tanaka et al. [42] and Wattenbarger et al. [43] showed that the surface chains take smaller conformational entropy in a confined state compared with that of bulk chains. The difference in conformational entropy between the surface chain and the bulk one, i.e. the conformational entropic penalty of the polymeric chain at the surface increases with  $M_n$  [43,44]. When the molecular weight of PMMA was increased from 102.6k to 387k (the  $2R_g$  of PMMA was increased from 18.0 to 35.0 nm), the PMMA38 chains absorbed on the SiO<sub>x</sub> substrate during spin-coating had more conformational entropic penalty than those of PMMA10. To reduce the system's free energy, the recovery of the conformational entropy loss of PMMA38 chains upon annealing will take place and lead to the PMMA chains aggregating.

#### 4. Conclusion

It was found that the dewetting of a PS film could be inhibited via addition of a low concentration of PMMA component. The effect of dewetting inhibition depends on the concentration and the molecular weight of PMMA component. By increasing the content of PMMA10 to 10.0 wt%, the dewetting of PS/PMMA10 blend film can be retarded to a great extent. Low and intermediate molecular weight PMMA1 and PMMA10 stabilize the films more effectively than a higher molecular weight PMMA38. The stabilizing effect can be mainly attributed to the preferential segregation of PMMA10 to the solid substrate and the formation of a nanometer thick PMMA-rich phase layer, which lower the interfacial tension between PS and PMMA. This may be a simple and low-cost method by using phase

separation property to control thin polymer film dewetting in applications.

#### Acknowledgements

This work is subsidized by the National Natural Science Foundation of China for General (20074037, 50027001, 20274050) and Major (50290090) Program and National Science Fund for Distinguished Young Scholars of China (59825113, 50125311), and the Ministry of Science and Technology of China for Special Pro-funds for Major State Basic Research Projects (2002CCAD4000) and the Special Funds for Major State Basic Research Projects (G1999064800). The authors also thank for the Chinese Academy of Sciences for Distinguished Talents Program and Intellectual Innovations Project (KGCX2-205-03), and Jilin Province for Distinguished Young Scholars Fund (20010101).

#### References

- [1] Kargupta K, Konnur R, Sharma A. *Langmuir* 2000;16:10243.
- [2] Russell TP. *Mater Sci Rep* 1990;5:171.
- [3] Wu S. *Polymer interfaces and adhesion*. New York: Marcel Dekker; 1982.
- [4] Geoghegan M, Krausch G. *Prog Polym Sci* 2003;28:261.
- [5] Akpalu YA, Karim A, Satija SK, Balsara NP. *Macromolecules* 2001;34:1720.
- [6] Krausch G. *Mater Sci Eng. Rep* 1995;R14:1.
- [7] Binder K. *Adv Polym Sci* 1999;138:1.
- [8] Budkowski A. *Adv Polym Sci* 1999;148:1.
- [9] Jones RAL, Norton LJ, Kramer EJ, Bates FS, Wiltzius P. *Phys Rev Lett* 1991;66:1326.
- [10] Bruder F, Brenn R. *Phys Rev Lett* 1992;69:624.
- [11] Krausch G, Dai CA, Kramer EJ, Bates FS. *Phys Rev Lett* 1993;71:3669.
- [12] Krausch G, Dai CA, Kramer EJ, Marko JF, Bates FS. *Phys Rev Lett* 1993;26:5566.
- [13] Krausch G, Kramer EJ, Rafailovich MH, Sokolov J. *Appl Phys Lett* 1994;64:2665.
- [14] Sung L, Karim A, Han CC. *Phys Rev Lett* 1996;76:4368.
- [15] Ermi BD, Karim A, Douglas JF. *J Polym Sci Polym Phys* 1998;36:191.
- [16] Karim A, Slawacki TM, Kumar SK, Douglas JF, Satija SK, Han CC, Russell TP, Liu Y, Overney R, Sokolov J, Rafailovich MH. *Macromolecules* 1998;31:857.
- [17] Steiner U, Klein J, Fetters L. *Phys Rev Lett* 1994;72:1498.
- [18] Genzer J, Kramer EJ. *Phys Rev Lett* 1997;78:4946.
- [19] Walheim S, Boltau M, Mlynec J, Krausch G, Steiner U. *Macromolecules* 1997;30:4995.
- [20] Müller-Buschbaum P, Gutmann JS, Stamm M. *Macromolecules* 2000;33:4886.
- [21] Oslanec R, Costa AC, Composto RJ, Vlcek P. *Macromolecules* 2000;33:5505.
- [22] Barnes KA, Karim A, Douglas JF, Nakatani AI, Gruell H, Amis EJ. *Macromolecules* 2000;33:4177.
- [23] Sharma S, Rafailovich MH, Peiffer D, Sokolov J. *Nano Lett* 2001;1:511.
- [24] Mackay ME, Hong Y, Jeong M, Hong S, Russell TP, Hawker CJ, Vestberg R, Douglas JF. *Langmuir* 2002;18:1877.



- [25] Orlicki JA, Moore JS, Sendjarevic I, McHugh AJ. *Langmuir* 2002;18:9985.
- [26] Tanaka K, Takahara A, Kajiyama T. *Macromolecules* 1996;29:3232.
- [27] Harris M, Appel G, Ade H. *Macromolecules* 2003;36:3307.
- [28] Reiter G. *Phys Rev Lett* 1992;68:75.
- [29] Reiter G. *Macromolecules* 1994;27:3046.
- [30] Reiter G. *Langmuir* 1993;9:1344.
- [31] Stage TG, Mathew R, Evens DF, Hendrickson WA. *Langmuir* 1992;8:921.
- [32] Sharma A, Reiter G. *J Colloid Interface Sci* 1996;178:383.
- [33] Qu S, Clarke J, Liu Y, Rafailovich MH, Sokolov J, Phelan KC, Krausch G. *Macromolecules* 1997;30:3640.
- [34] Krausch G. *J Phys: Condens Matter* 1997;9:7741.
- [35] Venugopal G, Krause S. *Macromolecules* 1992;25:4626.
- [36] Douglas JF. *Macromolecules* 1989;22:3707.
- [37] Yerushalmi-Rozen R, Klein J, Fetters LJ. *Science* 1994;263:793.
- [38] Calvert P. *Nature* 1996;384:311.
- [39] Sferrazza M, Xiao C, Jones RAL. *Phys Rev Lett* 1997;78:3693.
- [40] Brochard-Wyart F, Martin P, Redon C. *Langmuir* 1993;9:3682.
- [41] Hu H, Granick S. *Science* 1992;258:1339.
- [42] Tanaka K, Takahara A, Kajiyama T. *Macromolecules* 1998;31:863–9.
- [43] Wattenbarger MR, Chan HS, Evans DF, Bloomfield VA, Dill KA. *J Chem Phys* 1990;93:8343.
- [44] Sferrazza M, Xiao C, Bucknall DG, Jones RAL. *J Phys: Condens Matter* 2001;13:10269.